HAL
archives-ouvertes.fr

MULTI-TEXTURING 3D MODELS: HOW TO CHOOSE THE BEST TEXTURE?

Youssef Alj, Guillaume Boisson, Philippe Bordes, Muriel Pressigout, Luce Morin

To cite this version:

Youssef Alj, Guillaume Boisson, Philippe Bordes, Muriel Pressigout, Luce Morin. MULTI-TEXTURING 3D MODELS: HOW TO CHOOSE THE BEST TEXTURE?. IC3D, Dec 2012, Belgium. 2012. <hal-00785836>

HAL Id: hal-00785836

https://hal.archives-ouvertes.fr/hal-00785836

Submitted on 7 Feb 2013

HAL is a multi-disciplinary open access archive for the deposit and dissemination of scientific research documents, whether they are published or not. The documents may come from teaching and research institutions in France or abroad, or from public or private research centers.

L'archive ouverte pluridisciplinaire **HAL**, est destinée au dépôt et à la diffusion de documents scientifiques de niveau recherche, publiés ou non, émanant des établissements d'enseignement et de recherche français ou étrangers, des laboratoires publics ou privés.

MULTI-TEXTURING 3D MODELS: HOW TO CHOOSE THE BEST TEXTURE?

Youssef Alj, Guillaume Boisson, Philippe Bordes

Technicolor
1 avenue Belle Fontaine CS 17616
35576 Cesson-Sévigné Cedex
France

Muriel Pressigout, Luce Morin

INSA Rennes
20 avenue des Buttes de Coësmes
35043 Rennes Cedex
France

ABSTRACT

In this article, the impact of 2D based approaches for multi-texturing 3D models using real images is studied. While conventional 3D based approaches assign the best texture for each mesh triangle according to geometric criteria such as triangle orientation or triangle area, 2D based approaches tend to minimize the distortion between the rendered views and the original ones. Evaluation of the two strategies is performed on real scenes for two image sequences and results are provided using the PSNR metric. Moreover, an improvement of the image-based approach is proposed for texturing partially visible triangles.

***Index Terms*—** Multi-texturing, best texture, OpenGL, mesh, PSNR.

1. INTRODUCTION

Since the introduction of texture mapping in computer graphics in the mid seventies, acquiring photo realistic 3D models has become necessary for various applications such as cultural heritage, architecture and entertainment industry. Typically in such applications, one seeks to texture a 3D model given a set of photographs captured from various viewpoints. The straightforward approach for texturing the 3D model is to determine the best texture for each mesh facet. The point is then to find a criterion to define the best texture. 3D geometric criteria such as angle between the line of sight and the triangle orientation [3], distance to the viewing camera [2] or facet's area [8] may be considered to solve this problem. The aim of multi-texturing is to determine the texture providing the best rendering. To this end, photoconsistency based multi-texturing was introduced in [1]. It aims to assign for each mesh triangle the best texture by minimizing the 2D distortion, *i.e*. the quadratic error between the rendered and original views. Given these approaches, we attempt to address the following questions : what is the impact of an approach based on 2D distortion on the quality of the rendered views ? And do 2D approaches really add a significant improvement in terms of PSNR ? In this paper we present a comparison between texture selection using 3D geometric criteria and a 2D approach based on distortion minimization of the rendered images. This distortion is measured using the PSNR metric classically used within the video coding community. Actually, the PSNR metric is employed in order to evaluate fidelity between a reference and recovered image. In this study, this metric is used for both assigning the best texture to mesh triangles as well as for comparing geometric versus image based criteria for multi-texturing 3D models. The contributions of this paper are twofold :

- First, we study the impact, on the rendered views, of using geometric versus image based criteria for multi-texturing 3D models.
- Second, we extend the photoconsistency based multi-texturing method to handle partially visible triangles.

2. RELATED WORK

View Dependent Texture Mapping was first introduced by Debevec et al. in [3] with real time application in [4]. In this scheme, the user specifies a virtual view to render the mesh, and the best texture for each mesh triangle is chosen as the one the minimizes the angle between the triangle normal and the viewing directions of input cameras. For instance, when generating a novel view from the left, it would be better to use the image corresponding to the left view as the texture map. View Dependent Texture Mapping approaches consider the transmission of the set of all textures which requires a tremendous amount of data. The Floating Textures scheme [5] alleviates inaccuracies inherent to the geometric model and the camera calibration, and proposes a pairwise warping between input images using optical flow. Instead of using the optical flow, Harmonised Texture Mapping [9] used an optimized version of the input mesh in order to control the range of texture deformation. Lempitsky and Ivanov [8] formulate multi texturing the 3D model as a labelling problem : each texture should be assigned as a label to the mesh triangle. They expressed their labelling strategy as on energy minimi-

zation problem with two terms, the first one describing how better an input texture suits the triangle and the second one penalizing seams' visibility. Computation of the best texture per triangle is based on the angle between the viewing direction and the triangle normal. Based on energy minimization scheme, Gal *et al*. [6] extend the best texture search space to include a set of transformed images that compensate geometric errors and make use of Poisson blending to address lighting variation. The Unstructured Lumigraph Rendering method [2] uses a penalty function for each view in order to determine the best view for each triangle, this penalty is a linear combination of three terms : visibility constraints, the angle between the desired view to render and the set of input cameras and the resolution of the projected triangle. Other approaches form a single texture map by blending the available images. In [10], the unique texture map generation is presented as a super resolution problem [7]. The authors used image processing tools to compute the correct weights for blending. Finally, a 2D criterion for best texture selection is based on photoconsistency with the set of input images was first proposed in [1]. Their idea is based on distortion minimization between the rendered and original views. This distortion is measured in terms of quadratic error.

In this paper, we compare the impact of multi-texturing 3D models using geometric criteria, namely triangle orientation and triangle area, versus using 2D criterion based on photoconsistency on the other hand.

3. GEOMETRIC CRITERIA FOR MESH TEXTURING

Given a triangular mesh $\mathcal{M}$ and a set of texture images $\mathcal{I} = \{I_1, \ldots, I_n\}$. Each texture I_i is respectively captured from the views $\mathcal{V} = \{V_1, \ldots, V_n\}$. The aim is to find for each mesh triangle $t \in \mathcal{M}$ the best texture image $\hat{\mathrm{I}}_t \in \mathcal{I}$ using a geometric criterion C_k, where C_k could be one of the following criteria :

- $C_1 := \langle \vec{d}_j, \vec{n}_t \rangle$ *i.e.* dot product between triangle normal $\vec{n}_t$ and viewing direction (*i.e.* optical axis, that is image plane normal) $\vec{d}_j$ of the view V_j. Small angles between triangle normal and viewing directions of input cameras are then preferred. Note that in the case of parallel camera setup this criterion is not applicable.
- $C_2 := \langle \vec{e}_j, \vec{n}_t \rangle$, where $\vec{e}_j$ denotes the direction of the ray joining the triangle barycenter and the camera's position. Views where the triangle's viewing cone is larger are then preferred.
- $C_3 := \mathrm{area}_j(t)$ the area of the projected triangle onto the view V_j. Views where the resolution of the projected triangle is larger are then preferred.

Let $P_j(t)$ denote the projection of triangle t onto the view V_j. $P_j(t)$ consists in a set of pixels (q, l) corresponding to the rasterization of triangle t, *e.g.* using *OpenGL* rendering engine. The best texture $\hat{\mathrm{I}}_t$ is computed the following way : first

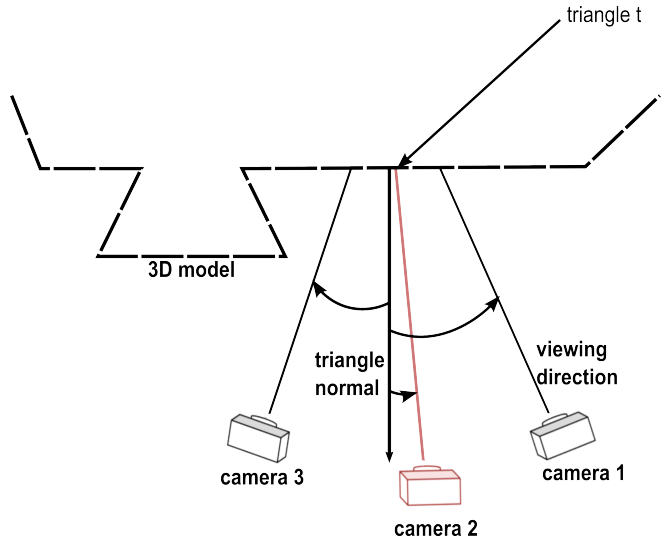

Fig. 1. Best texture selection as the minimizer of the angle between the triangle normal and cameras viewding direcions.

for each triangle t, total and partial visibility are determined with respect to each view. The best texture is then determined as the maximizer of C_k with respect to visibility constraints. Figure 1 illustrates the principle of best texture selection using C_1. This figure shows that the best view to texture the triangle t is the camera 2. Indeed, the angle between the viewing direction of the camera 2 and the triangle normal is minimum, which corresponds to a maximum dot product.

3.1. Visibility determination

Given the input mesh $\mathcal{M}$, total and partial visibility are first determined for each triangle with respect to each view. At the end of this step, each triangle will have one of the three labels per view : "totally visible", "partially visible" or "hidden". The algorithm is detailed in the next section.

3.1.1. Total visibility

In this step only the labels "totally visible" and "hidden" are assigned to mesh triangles. The status of each mesh triangle is initialized to "totally visible". The visibility of each triangle is determined by computing the visibility of the triangle vertices. A triangle is marked as hidden if at least one of its vertices is hidden. Vertex visibility with respect to each camera is determined using OpenGL z-buffer denoted as Z^j_{buffer} (*i.e.* z-buffer of the mesh projected onto the view V_j). During the first pass, the input mesh is projected onto the current view, and the z-buffer is extracted. The second pass is dedicated to vertex visibility determination using the computed z-buffer. Each mesh vertex is projected onto the current view and the depth component, denoted as $z_{\mathrm{projected}}$, is checked

against the pixel depth $Z^j_{\text{buffer}}[q,l]$. If the projected vertex is behind the pixel in the z-buffer, then this vertex is hidden, and thus the set of mesh triangles sharing this vertex are marked hidden. The pseudo-code for total visibility determination is provided in algorithm 1.

Algorithm 1: Global visibility determination.

```
// Views traversal
for each view V_j do
    Initialize all triangles to visible.
    Project the M onto V_j.
    Store the depth buffer Z^j_buffer.
    // Mesh vertices traversal
    for each vertex v do
        Determine (q, l, z_projected) the projection of the
        vertex v onto V_j.
        if Z^j_buffer[q, l] > z_projected then
            v is a hidden vertex.
            Mark all the triangles lying on v as hidden.
```

3.1.2. Partial visibility

Until now, each triangle has one of the two labels : "totally visible" or "hidden". At the end of this step, "hidden" triangles will be sorted out as "partially visible" or totally "hidden". To this end the depth of each pixel is checked against the stored depth buffer in the projected triangle. Note that it is necessary to check the depth of the projected triangle. Partial visibility determination by counting the number of hidden vertices is not sufficient as some triangles could be partially visible and have a number of hidden vertices of three. The algorithm determining partial visibility is presented in algorithm 2.

Algorithm 2: Partial visibility determination.

```
// Views traversal
for each view V_j do
    // Mesh triangles traversal
    for each triangle t do
        if triangle t is hidden in V_j then
            Determine P_j(t) the projection of triangle t
            onto V_j.
            for each pixel (q, l) in P_j(t) do
                Get the pixel depth z.
                if z == Z^j_buffer[q, l] then
                    Mark t as partially visible in V_j.
```

3.2. Best texture computation using geometric criterion

In this section the best texture is assigned to the set of triangles which are totally or partially visible using one of the three criteria discussed above. Algorithm 3 describes how the best texture is assigned for such triangles. The user specifies a geometric criterion C_k. The view that maximizes C_k is assigned as the best texture for the current triangle.

Algorithm 3: Best texture determination using C_k.

```
// Triangles traversal
for each triangle t do
    Get the normal of the triangle t.
    // Views traversal
    for each view V_j do
        if t is visible or partially visible in V_j then
            Compute C_k.
    Compute Î_t which maximizes C_k
```

4. PHOTO-CONSISTENCY BASED MESH TEXTURING

Photoconsistency based mesh texturing was first introduced in [1]. Figure 2 illustrates the photoconsistency principle. The triangle t is visible in cameras 1, 2, 3. For each texture $I_i \in \mathcal{I}$, the triangle t is textured with texture I_i (red arrow for texture mapping operation) and projected (green arrow for projection operation) onto the cameras 1, 2, and 3 - i.e. the set of cameras where t is visible. The error of texturing the triangle t with each available texture is computed. This error is referred to as the photoconsistency metric. The best texture is chosen as the minimizer of the photoconsistency metric. In [1] only totally visible triangles are addressed, and partially visible ones are textured using the view of the frontal camera. The novelty of the approach described in this paper is to extend the photoconsistency-based best texture computation for partially visible triangles too. The overall framework is sketched in Figure 3. First, visibility is determined for each triangle with respect to each view. Second, each available texture is mapped on visible triangles of the input mesh. Photometric projection error is computed for each triangle and for each input view and stored in distortion images. Synthesized views are produced by rendering the textured mesh, each triangle being textured with the best texture according to the photoconsistency metric. In the next section each step of this algorithm is described in more details.

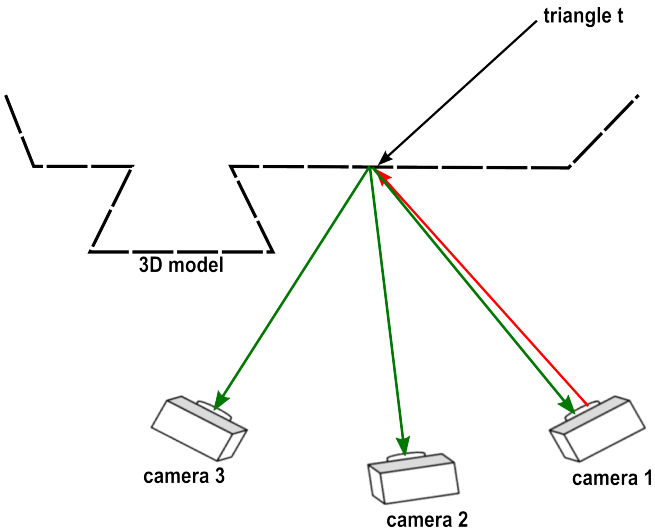

Fig. 2. Best texture determination using photoconsistency. Red arrow for texture mapping operation and green arrow for projection operation.

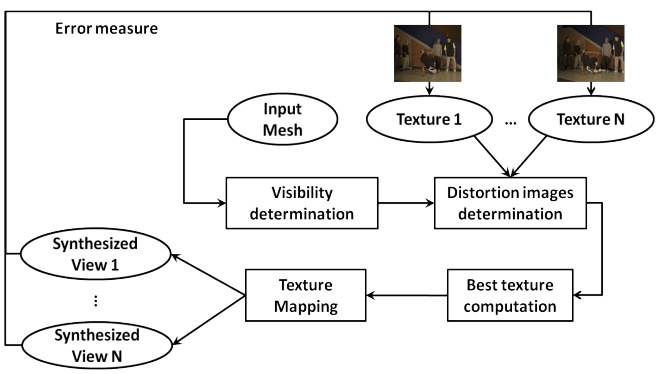

Fig. 3. Overall framework.

4.1. Distortion images determination

In order to determine the error of texturing a triangle with an input texture I_i, each available texture is then mapped on the merged mesh and projected onto each camera. Let $P_j^i(\mathcal{M})$ be the projection of the mesh $\mathcal{M}$ onto the view V_j textured with the image I_i. For each available texture the following distortion image is computed in RGB color space :

$$D_{i,j} = \|P_j^i(\mathcal{M}) - I_j\|_2$$

4.2. Best texture determination

In this section, the best texture is chosen for each mesh triangle using the distortion images. The best texture for each triangle relies on the computed set of pixels that belong to the projected triangle and visible in the current view V_j, i.e. the set of pixels :

$$\mathrm{Vis}_j(t) = \{(q,l) \in P_j(t), (q,l) \text{ visible in } V_j\}$$

Figure 4 shows how $\mathrm{Vis}_j(t)$ is determined for partially and totally visible triangles. The grid represents image pixels. In 4(a) the blue triangle is totally visible, the set of pixels defining $\mathrm{Vis}_j(t)$ are shown in red. On the contrary, the blue triangle in 4(b) is partially visible as it is occluded by the green triangle. $\mathrm{Vis}_j(t)$ in this case is restricted to the non-occluded pixels. The photoconsistency metric is then computed for each triangle with respect to $\mathrm{Vis}_j(t)$. This metric measures the error of texturing the triangle t with the texture image I_i. From here on, for sake of simplicity, visible triangle will refer to totally or partially visible triangle as they will be treated the same way.

$\forall i \in \{1, \ldots, n\}$ we compute :

$$\mathcal{E}_{t,I_i} = \sum_{\substack{j=1 \\ t \text{ visible in } V_j}}^{n} \left(\sum_{(q,l)\in \mathrm{Vis}_j(t)} D_{i,j}[q,l] \right) ,$$

The best texture for a visible triangle t is then given by :

$$\hat{I}_t = \arg\min_{I_i \in \mathcal{I}} \mathcal{E}_{t,I_i} .$$

The steps of best texture computation are summarized in algorithm 5.

Algorithm 4: Compute distortion images.

```
// Textures traversal
for each texture I_i do
    // Views traversal
    for each view V_j do
        Compute P_j^i(M) : projection of the mesh
        textured with texture I_i onto view V_j.
        D_{i,j} = ||P_j^i(M) - I_j||_2
```

Algorithm 5: Compute the best texture for each triangle.

```
// Triangles traversal
for each triangle t do
    // Views traversal
    for each view V_j do
        Determine Vis_j(t).
    // Textures traversal
    for each texture I_i do
        Compute E_{t,I_i}.
    Determine Î_t.
```

4.3. Texture mapping

Finally, the views are rendered. The 3D model is projected according to the camera's parameters supplied by the user. Then each triangle is textured using the texture coordinates determined during visibility determination step.

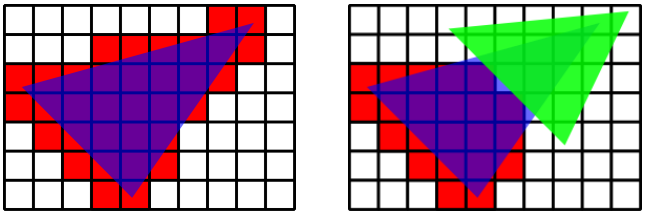

(a) total visibility (b) partial visibility

Fig. 4. Best texture computation. Handling partial/global visibility.

5. IMPLEMENTATION AND RESULTS

Results are presented for two sequences *breakdancers* and *balloons*. Breakdancers, provided by Microsoft, is captured by eight convergent cameras. Balloons sequence, provided by Nagoya University, is captured by three parallel cameras. Both sequences have XGA resolution (1024x768). The geometric model used in this study is based on the 3D reconstruction scheme presented in [1].

Results of the rendered views are provided in figure 6 and in figure 5. It can be seen that photoconsistency based mesh texturing provides better visual quality than geometric based methods. More precisely, in figure 5, the frontier between the two brown walls is well-aligned using the photoconsistency criterion, while this frontier is misaligned using the geometric criterion. Besides, the floor appears to be noisy using geometric criterion, while it is much smoother using the photoconsistency criterion. Figure 7 shows that the difference in terms of PSNR between photoconsistency criterion and any other geometric criterion is noticeable (the average difference is at least 1dB between the two methods).

Regarding the photoconsistency criterion, results also show that PSNR is higher for cameras near the frontal camera (see Figure 7), which is due to the large number of triangles assigned to the texture of the frontal camera. However, photoconsistency based multi-texturing algorithm is time-consuming (about 10x more) comparing to geometric methods. Therefore it turns out that photoconsistency based multi-texturing is best suited for offline rendering. These results suggest the use of the photoconsistency based multi-texturing for transmission purposes where distortion minimization is often a key element to take into account.

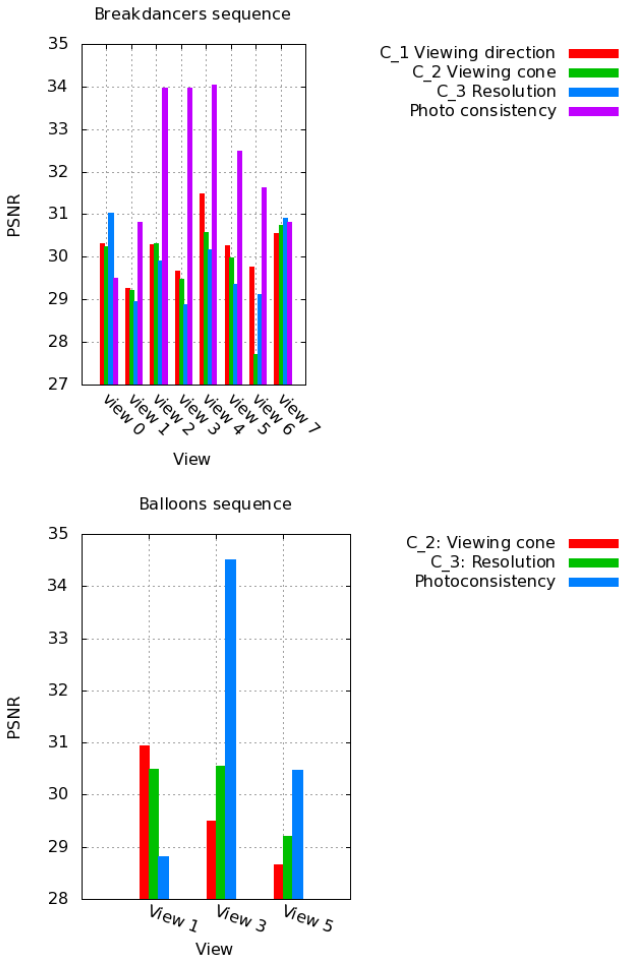

Fig. 7. PSNR evolution through different views using different criteria for Breakdancers and Balloons sequences.

6. CONCLUSION

In this paper, multi-texturing 3D models was addressed by considering several criteria for best texture assignment to mesh triangle. Conventional geometric criteria assign the view that minimizes the angle between the viewing direction and the triangle normal, or the view that maximizes the triangle resolution. On the contrary, 2D based approaches minimize the distortion between the rendered views and the original ones. We show that photoconsistency based methods are significantly more relevant for transmission purposes. Indeed they outperform geometric based methods both in terms of objective and subjective visual quality of synthesized views. The PNSR gap exceeds 2dB for the common test-sequences. As a perspective, we plan to investigate how to reduce complexity without altering too much the quality of the synthesized views. We also aim to improve spatial consistency of the assigned textures in order to reduce the coding cost of the

texture signal.

7. REFERENCES

[1] Y. Alj, G. Boisson, P. Bordes, M. Pressigout, and L. Morin. Space carving mvd sequences for modeling natural 3d scenes. volume 8290, page 829005. SPIE, January 2012.

[2] C. Buehler, M. Bosse, L. McMillan, S. Gortler, and M. Cohen. Unstructured lumigraph rendering. In *Proceedings of the 28th annual conference on Computer graphics and interactive techniques*, pages 425–432. ACM, 2001.

[3] P.E. Debevec, C.J. Taylor, and J. Malik. Modeling and rendering architecture from photographs : A hybrid geometry-and image-based approach. In *Proceedings of the 23rd annual conference on Computer graphics and interactive techniques*, pages 11–20. ACM, 1996.

[4] P.E. Debevec, Y. Yu, and G. Borshukov. Efficient view-dependent image-based rendering with projective texture-mapping. In *Eurographics Rendering Workshop*, volume 98, pages 105–116, 1998.

[5] Martin et al. Eisemann. Floating textures. *Computer Graphics Forum (Proc. of Eurographics)*, 27(2) :409–418, April 2008.

[6] R. Gal, Y. Wexler, E. Ofek, H. Hoppe, and D. Cohen-Or. Seamless montage for texturing models. In *Computer Graphics Forum*, volume 29, pages 479–486. Wiley Online Library, 2010.

[7] M. Iiyama, K. Kakusho, and M. Minoh. Super-resolution texture mapping from multiple view images. In *Pattern Recognition (ICPR), 2010 20th International Conference on*, pages 1820–1823. Ieee, 2010.

[8] V. Lempitsky and D. Ivanov. Seamless mosaicing of image-based texture maps. In *Computer Vision and Pattern Recognition, 2007. CVPR'07. IEEE Conference on*, pages 1–6. IEEE, 2007.

[9] T. Takai, A. Hilton, and T. Matsuyama. Harmonised texture mapping. In *Proc. of 3DPVT*, 2010.

[10] L. Wang, S.B. Kang, R. Szeliski, and H.Y. Shum. Optimal texture map reconstruction from multiple views. In *Computer Vision and Pattern Recognition, 2001. CVPR 2001. Proceedings of the 2001 IEEE Computer Society Conference on*, volume 1, pages I–347. IEEE, 2001.

(a) Original image camera 7

(b) Zoom on original image camera 7

(c) Synthesized image camera 7 using viewing cone criterion C_2

(d) Zoom on synthesized image camera 7 using viewing cone criterion C_2

(e) Synthesized image camera 7 using photoconsistency

(f) Zoom on synthesized image camera 7 using using photoconsistency

Fig. 5. Rendered images for breakdancers sequence using viewing cone criterion vs. photoconsistency.

(a) Original image camera 5

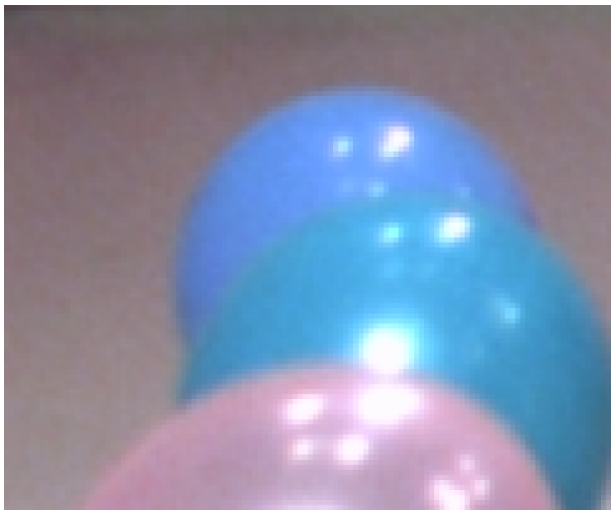

(b) Zoom on original image camera 5

(c) Synthesized image camera 5 using triangle resolution criterion C_3

(d) Zoom on synthesized image camera 5 using triangle resolution criterion C_3

(e) Synthesized image camera 5 using photoconsistency

(f) Zoom on synthesized image camera 5 using photoconsistency

Fig. 6. Rendered images for balloons sequence using resolution criteria versus photoconsistency.